PHILOSOPHICAL TRANSACTIONS OF THE ROYAL SOCIETY A MATHEMATICAL, PHYSICAL & ENGINEERING SCIENCES

Petrology of a Transform Fault Zone and Adjacent Ridge Segments

W. G. Melson and G. Thompson

Phil. Trans. R. Soc. Lond. A 1971 **268**, 423-441
doi: 10.1098/rsta.1971.0005

Phil. Trans. Roy. Soc. Lond. A. **268**, 423–441 (1971) [423]
Printed in Great Britain

Petrology of a transform fault zone and adjacent ridge segments

By W. G. Melson
Smithsonian Institution, Washington, D.C. 20560

and G. Thompson
Woods Hole Oceanographic Institution, Woods Hole, Massachusetts 02543

[Plate 4]

The Vema Fracture Zone in the North Atlantic (9 to 11° N), which has been identified as a transform fault zone, contains exposures of serpentinized peridotites, while its adjacent ridge segments are floored mainly by typical abyssal ocean ridge basalts. This petrologic contrast correlates with the greater frequency of volcanic eruptions along the actively spreading ridge segments compared to the transform fault zone. Where rifting components occur across transform faults, exposures of the deeper zone of oceanic crust may result. The bathymetry of the Vema Fracture Zone suggests that some uplift parallel to the fracture zone as well as rifting led to exposures of deeper rocks. The basalts from the adjacent ridge axes contain 'xenocrysts' of plagioclase and olivine and more rarely of chromite. These appear to have a cognate origin, perhaps related to cooling and convection in near surface magma chambers. The basalts from the ridge axes, offset and on opposite sides of the transform fault, have similar features and compositions. The plagioclase peridotites have mineralogical features which indicate equilibration in the plagioclase pyrolite facies, suggesting maximum equilibration depths of around 30 km for a temperature of around 1200 °C. The chemical characteristics of the Vema F.Z. peridotites suggest that they may be undifferentiated mantle, emplaced as a subsolidus hot plastic intrusion or as a crystal mush. The abundance of peridotites and serpentinized peridotites is believed to reflect their abundance in seismic layer three of the oceanic crust.

Background

A number of petrologic models have been proposed for the oceanic crust. These commonly divide the hard rocks of the oceanic crust into two zones which correlate roughly with seismic layers two and three. The upper zone is undoubtedly mainly volcanic rocks formed by basaltic eruptions along actively spreading ridge crests. The constitution of the lower zone is debated. Hess (1962, 1965) among others postulated that it is mainly serpentinite. Cann (1968) and Miyashiro, Shido & Ewing (1970, and this volume, p. 589) suggest that it is mainly metabasic rocks, the lower zone being mainly amphibolites. Others (see, for example, Melson 1968; Thompson, Melson & Bowen 1970) have postulated that it is a mixture of various basic and ultrabasic plutonic and metamorphic rocks and that its constitution may differ from place to place along the mid-ocean ridges and fracture zones. Without deep crustal drilling, there appears to be no way to categorically choose between these various models. All are designed to be consistent with existing geophysical data.

The present study examines the detailed features of rock samples from a fracture zone and its adjacent ridge segments. About 11° N, the Mid-Atlantic Ridge is intersected and appears offset by more than 300 km in a left-lateral sense. This zone of offset has been the subject of detailed bathymetric studies and interpretations by van Andel and his co-workers (1967, 1969), and has been identified as a major transform fault zone by Sykes (1967). The distinctly different tectonic settings between ridge segments and transform fault zones are now well known. On the ridge segments, rift faulting and abundant eruptions occur and accompany sea-floor spreading, while along transform fault zones, great blocks slide past one another as they move

away from the ridge crests (figure 1). Components of rifting have been postulated to occur across the Vema F.Z. due to a slight change in spreading directions along adjacent ridge segments (figure 2) and there has been some uplift parallel to the fracture (van Andel *et al.* 1967, 1969; van Andel 1969).

These different tectonic settings have been found to correlate with important petrologic differences in the Vema F.Z. and adjacent ridge segments. Fresh basalts occur along the normal

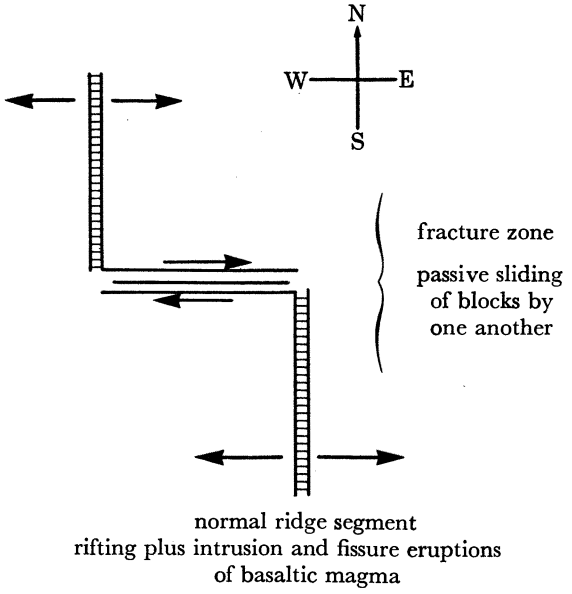

FIGURE 1. Simplified comparison of tectonic movements at idealized normal ridge segments and at fracture zones.

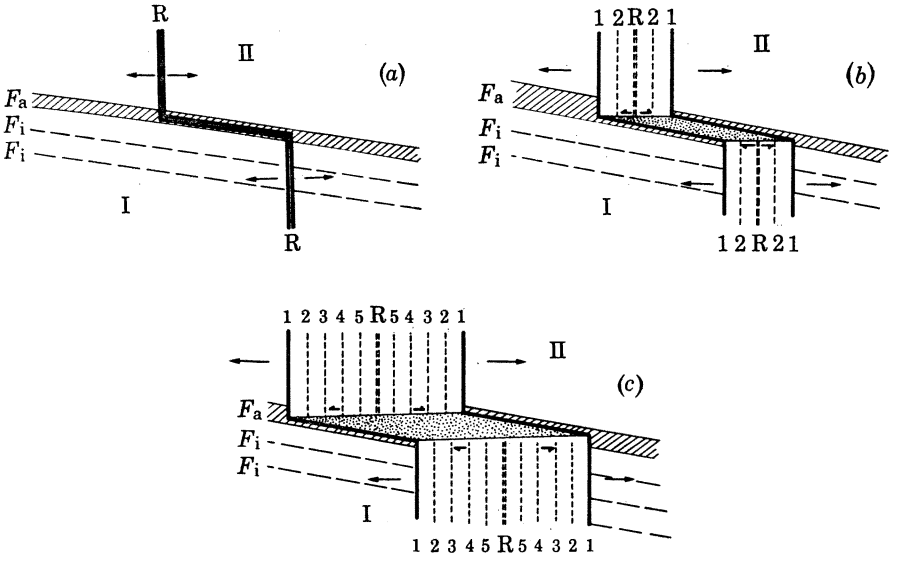

FIGURE 2. Model proposed by van Andel *et al.* (1969) to explain rift features of the Vema Zone. Stage (*a*) shows incipient movement by spreading at two ridge crests (R) offset along an old fracture zone (F_a) trending at an angle to the new direction of spreading. Other old fractures (F_i) are inactive. Progressive spreading and formation of new crusts (stages (*b*) and (*c*)) produces an open rift (stippled area) along old fracture line. Successive growth stages of new crust on ridge crust indicated by numbers. The heavy line marks the initial boundaries of blocks I and II.

PHILOSOPHICAL TRANSACTIONS OF THE ROYAL SOCIETY A MATHEMATICAL, PHYSICAL & ENGINEERING SCIENCES

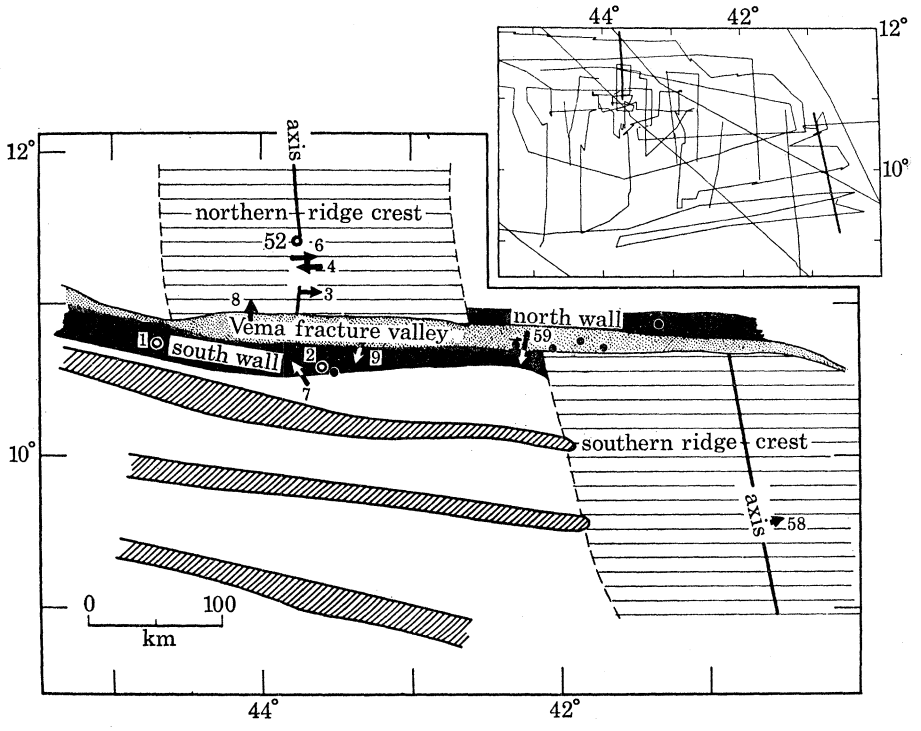

FIGURE 3. Dredge stations (arrows point upslope) and dart core stations. Diagonal hatchings are inactive fracture zones. →, dredge; ○, core; ●, earthquake epicentres.

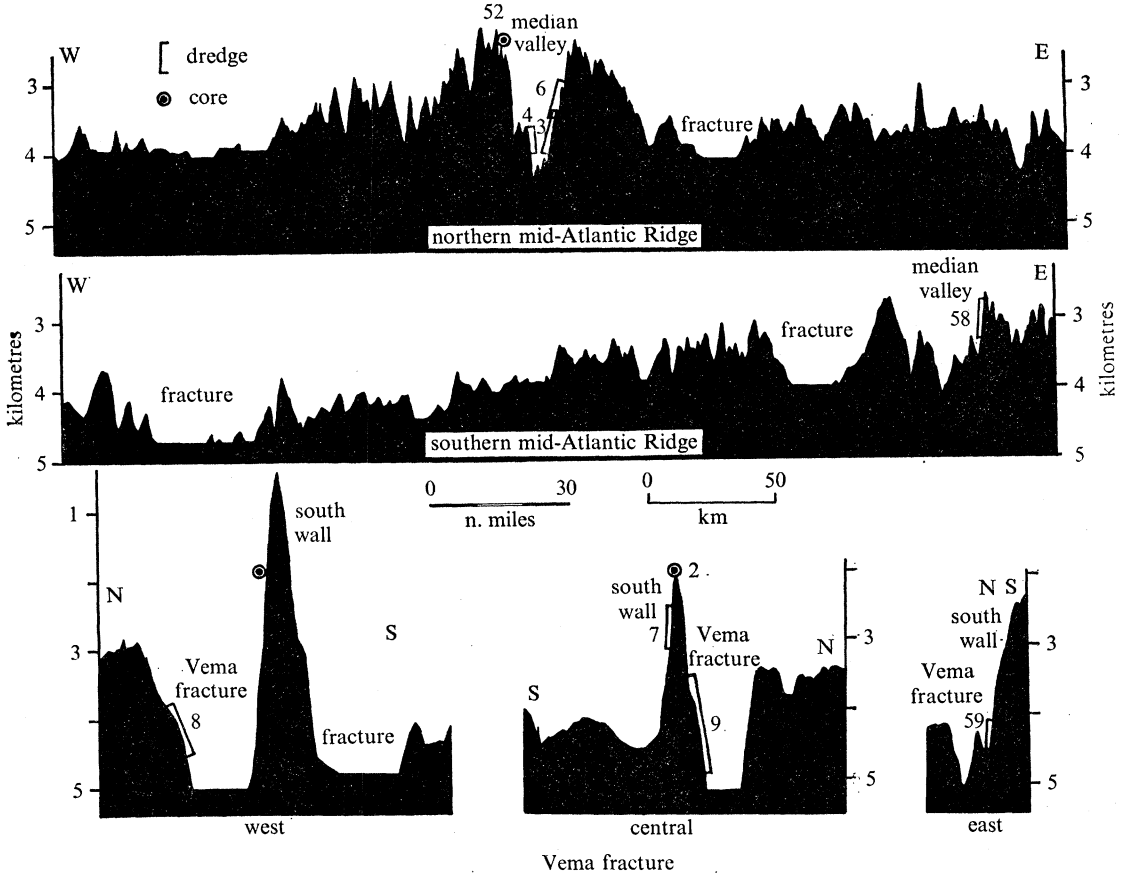

FIGURE 4. Profiles of dredge stations. Dredge stations are projections on the indicated profiles (modified from van Andel *et al.* 1967) and thus are not the actual dredge stations. Locations of profiles: top, 45° 28′ W, 11° 32′ N to 41° 53′ W, 11° 34′ N; centre, 43° 46′ W, 8° 54′ N to 40° 10′ W, 9° 25′ N; bottom left, 44° 20′ W, 11° 19′ N to 44° 28′ W, 10° 04′ N; bottom centre, 42° 35′ W, 11° 21′ N to 42° 09′ W, 10° 08′ N; bottom right, 41° 17′ W, 10° 55′ N to 41° 12′ W, 10° 33′ N. Vertical exaggeration, 27 times.

ridge segments north and south of the zone (figure 3). Within the fracture zone, we have found that (1) basalts occur but that they are variously highly weathered and encrusted with thick Mn–Fe oxide rinds, or metamorphosed, or are doleritic and (2) serpentinized peridotites occur. The dredge stations and profiles of dredged slopes are in figures 3 and 4. The rock types, depth, and location of each dredge and dart core station are in table 1.

TABLE 1. ROCK SAMPLING STATIONS AND LOCATIONS, VEMA F.Z., 9 TO 11° N LATITUDE

station	gear	latitude	longitude	depth† m	topography	result
AII–20–3	rock dredge	11° 05′ N to 11° 02′ N	43° 42′ W to 43° 39.5′ W	4750 –3420	east wall of median valley	xenocrystal and platy basalts, with glassy margins and vesicles, some quenched on two sides (figure 6). One analysed basalt (table 3)
AII–20–4	rock dredge	11° 14′ N to 11° 15′ N	43° 42′ W to 43° 45′ W	4365 –3950	west wall of median valley	few fragments of glassy basalt
AII–20–6	rock dredge	11° 19′ N to 11° 14′ N	43° 41′ W to 43° 37′ W	4460– 3095	east wall of median valley	xenocrystal basalts, many with glassy margins. One analysed basalt (table 3)
AII–20–7	rock dredge	10° 33′ N to 10° 34.5′ N	43° 44.5′ W to 43° 44.5′ W	3000– 2270	south wall of Vema Fracture	few weathered basalt fragments
AII–20–8	rock dredge	10° 57.5′ N to 11° 02′ N	44° 05′ W to 44° 08′ W	4790– 3910	north wall of Vema Fracture	a few basalt and serpentinite fragments
AII–20–9	rock dredge	10° 44′ N to 10° 42′ N	43° 10′ W to 43° 25′ W	4990– 3490	south wall of Vema Fracture	serpentinized peridotite (figure 8 and table 7)
AII–20–58	rock dredge	09° 36′ N to 09° 37′ N	40° 39′ W to 40° 33′ W	3340– 2475	east wall of median valley	glassy and xenocrystal basalts (figure 7). One analysed basalt (table 3)
AII–20–59	rock dredge	10° 45′ N to 10° 43′ N	42° 16′ W to 42° 17′ W	4910– 4140	south wall of Vema Fracture	small fragment of coarse-grained basalt; fragments of amphibole-epidote-sphene rock; some ultramafic rock fragments
AII–20. Core 52	dart‡ core	11° 25′ N	43° 44′ W	2850	west wall of median valley	foraminiferal ooze overlying basalt
AII–31. Core 1	dart‡ core	10° 47.5′ N	44° 45′ W	2110	south wall of Vema Fracture	thick ferromanganese crust on palagonite
AII–31. Core 2	dart‡ core	10° 37.5′ N	43° 36.5′ W	1910	south wall of Vema Fracture	metabasalt (greenstone facies)

† Corrected for the velocity of sound in water.
‡ A dart core is essentially a high mass, high velocity gravity core which is allowed to 'punch' through the sediment cover and recover a small sample of the underlying rock.

Previous to the present study, differences between the petrology of normal ridge segments and fracture zones had been noted (Miyashiro, Shido & Ewing 1969*b*, 1970; Melson, Thompson & van Andel 1968). Fracture zones have been found to contain greater abundances of plutonic and metamorphic rocks than adjacent ridge crests (table 2). This relationship may be interpreted in one of two major ways (figure 5). At the present time we favour the view that fracture zones provide windows into the deeper zones of the oceanic crust (model I, figure 5). By this hypothesis, ultramafic rocks would appear to be a major component of the lower oceanic crust in the Vema F.Z.

TABLE 2. SOME REPORTED ROCK TYPES FROM CROSS-FRACTURES IN MID-OCEAN RIDGES

locality†	source	rock type
Mid-Atlantic Ridge		
43° N, 29° W	Phillips *et al.* (1969)	serpentinized peridotite. Fresh tholeiitic basalts recovered from median valley of ridge segment south of the cross-fracture
24° N, 46° W	Miyashiro *et al.* (1969)	serpentinites, serpentinized peridotite, weathered basalts and metabasalts. Fresh tholeiitic basalts recovered from median valley of ridge segment north of cross-fracture
30° N, 42° W (Atlantis F.Z.)	Miyashiro *et al.* (1969)	serpentinites, serpentinized peridotites, weathered basalts and metabasalts. Fresh tholeiitic basalts were recovered from the floor of the junction of median valley with the fracture zone
10° N, 43° W (Vema F.Z.)	this paper	serpentinized peridotite, weathered basalt, metabasalt. Fresh tholeiitic basalts recovered from median valley of ridge segments to north and south of the fracture
1° N, 29° W (St Paul F.Z.)	Melson *et al.* (1967*a*, *b*)	serpentinized peridotite, mylonitized peridotite, gabbros, basalts (alkaline and tholeiitic), metabasalts
	Bonatti (1968)	serpentinized peridotite, mylonitized peridotite, gabbro, basalt
0° N, 18° W (Romanche F.Z.)	Melson & Thompson (1970)	serpentinized peridotite, peridotite, gabbro (including layered gabbro), basalt, metabasalt, uralitized basalt
	Bonatti (1968)	serpentinized peridotite, gabbro, basalt, metabasalt
	Bogdanov & Ploshko (1968), Ploshko & Bogdanov (1968)	serpentinized peridotite, peridotite, gabbro, norite, basalt, metabasalt, amphibolite
1° S, 15° W (Chain F.Z.)	Bonatti (1968)	serpentinite and serpentinized peridotite
4° S, 12° W	Thompson *et al.* (1969)	serpentinized peridotite. Basalt and metabasalt recovered from junction of ridge segment and cross fracture
Mid-Indian Ocean Ridge		
5° N, 61° E	Cann & Vine (1966)	brecciated basalts and metabasalts
13° N, 66° E	Engel & Fisher (1969)	gabbros, peridotite and serpentinized peridotite
17° N, 66° E	Engel & Fisher (1969)	diabase, gabbros, anorthosite, peridotite and serpentinized peridotite. Fresh tholeiitic basalts recovered in median valley of ridge segments of mid-Indian Ocean ridge
33° S, 101° E (Diamentina F.Z.)	Hekinian (1968)	gabbro fragments in cored sediment
20° S, 61° E	Hekinian (1968)	serpentinized peridotite fragments in cored sediment
Pacific Ocean		
44° N, 130° W (Blanco F.Z.)	Melson (1970)	fresh and weathered basalts, metabasalts
	Duncan, in Vine & Hess (1970)	peridotite

† Localities rounded to nearest degree.

PHILOSOPHICAL TRANSACTIONS OF THE ROYAL SOCIETY A MATHEMATICAL, PHYSICAL & ENGINEERING SCIENCES

The following data centre on the petrographic and chemical characteristics of the fracture zone serpentinized peridotites and of the fresh basalts from the adjacent ridge crests. Major, minor and trace element analyses are given for one ultramafic and three basaltic rocks which are considered representative of the many samples studied. Selected electron probe analyses are given for these and other samples.

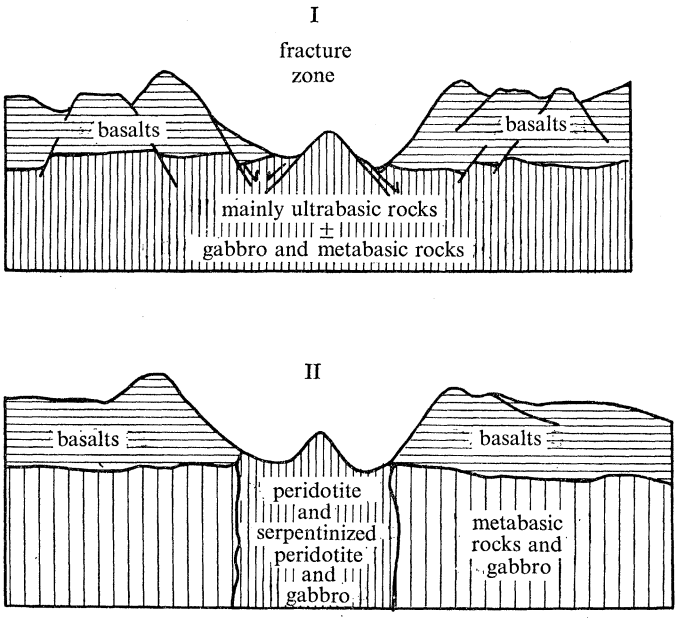

FIGURE 5. Alternative explanations for the abundance of ultrabasic and basic rocks in fracture zones. If model I is correct, then the constitution of the lower crust is revealed by fracture zone samples. If model II is correct, we have no samples of the lower crust; the lower crust of the fracture zones differ from the lower crust of normal ridge segments. Modified from Miyashiro *et al.* (1969).

BASALTS

Macroscopic features

Submarine basaltic eruptives in unmetamorphosed, unweathered condition can be divided into three eruptive facies: (1) pillow lavas, (2) sideromelane-rich tuffs, and (3) massive, essentially holocrystalline basalts (Melson *et al.* 1968). The latter rocks commonly have doleritic grain sizes (0.5 to 2.0 mm) and may be from thick flow interiors, lava lake interiors, or from dykes and sills. Only pillow lava fragments were recovered in the ridge segments north and south of the fracture zone, whereas coarser grained massive basaltic fragments were found within the fracture zone (dredge 59, figure 3) near the base of the south wall where they are associated with fragments of ultramafic rocks. These coarse grained basalts and a finer grained basalt (A1131–DC–2) from the top of the south wall have been partially to completely altered to chlorite–albite–actinolite–sphene greenstones. Scattered shear planes in the greenstones indicate that some faulting accompanied the low-grade metamorphism. Such greenstones are not restricted to fracture zones and have been found along normal undisrupted ridge segments (Melson *et al.* 1968). Cann (1969) has reviewed occurrences of similar rocks in the ocean basins and discussed their probable conditions of metaphorphism.

Pillow lava fragments from the mid-ocean ridges appear to be of at least two types: (1) actually

pillow-shaped to ovoid fragment, commonly with radial jointing and one outer quenched surface, and (2) thin platy pieces with quenched surfaces on two sides. The second variety is rare, but has been noted on the East Pacific Rise (Bonatti 1968) and from a basalt-floored median graben on the Juan de Fuca Ridge, Northeast Pacific (Melson 1970). We have found

TABLE 3. CHEMICAL COMPOSITION OF FRESH BASALTS FROM THE VEMA F.Z., AND AN AVERAGE ABYSSAL THOLEIITIC BASALT

	(1)	(2)	(3)	(4)
SiO_2	50.07	50.06	50.14	49.21 ± 0.74
Al_2O_3	17.67	15.76	15.90	15.81 ± 1.50
Fe_2O_3	1.33	1.63	1.42	2.21 ± 0.74
FeO	7.76	8.52	9.53	7.19 ± 1.25
MgO	6.58	7.87	7.33	8.53 ± 1.98
CaO	11.25	11.13	10.57	11.14 ± 0.78
Na_2O	2.79	2.79	2.95	2.71 ± 0.19
K_2O	0.12	0.12	0.11	0.26 ± 0.17
H_2O^+	0.31	0.44	0.23	—
H_2O^-	0.10	0.16	0.13	—
TiO_2	1.48	1.45	1.24	1.39 ± 0.28
P_2O_5	0.08	0.09	0.16	0.15 ± 0.04
MnO	0.15	0.17	0.20	0.16 ± 0.03
Total	99.69	100.19	99.91	
B	10	10	10	7 ± 3
Ba	7	9	5	12 ± 8
Cr	280	290	250	296 ± 80
Cu	70	75	70	87 ± 26
Ga	17	14	14	18 ± 5
Li	8	9	9	8 ± 5
Ni	100	130	100	123 ± 56
Pb	2	2	< 2	
Sr	150	110	100	123 ± 46
V	300	290	390	289 ± 73
Y	36	35	40	43 ± 12
Zn	145	140	125	122 ± 21
Zr	120	90	160	100 ± 42
		C.I.P.W. norms		
OR	0.71	0.71	0.77	—
AB	23.61	23.61	27.08	—
AN	35.34	30.13	28.64	—
Di	16.30	19.97	18.69	—
HY	15.70	13.88	9.30	—
OL	2.70	5.97	10.56	—
MT	1.93	2.36	2.06	—
IL	2.81	2.75	2.36	—
AP	0.19	0.21	0.37	—

(1) USNM 111308. Original no. AII–20–58–27. Highly porphyritic olivine basalt. Phenocrysts of plagioclase, olivine, and rarely chromite. Many crystals have rounded, resorbed appearance; others are euhedral.

(2) USNM 111327. Original no. AII–20–6–17. Pillow basalt with glassy rind. Very rare (1%) rounded micro-phenocrysts of olivine and plagioclase.

(3) USNM 111273. Original no. AII–20–3–5. Basalt with glassy rind. Rare microphenocrysts.

(4) Average and standard deviation for major and minor elements of 33 basalts dredged from greater than 1 km on the mid-Atlantic Ridge (Melson *et al.* 1968). New trace element average and standard deviation based on previously published data for oceanic tholeiitic basalts.

Major and minor elements determined by classical methods, E. Jarosewich, analyst; trace elements by direct-reading spectrometric methods, G. Thompson, analyst. Details of the method including precision and accuracy have been reported (Thompson & Bankston 1969). The following elements were sought but if present were below their detection limits (parts/10^6): Ag (< 1), Bi, Cd (< 2); Mo, Sn (< 5); Rb (< 20).

PHILOSOPHICAL TRANSACTIONS OF THE ROYAL SOCIETY A MATHEMATICAL, PHYSICAL & ENGINEERING SCIENCES

such fragments (figure 6, plate 4) in a dredge from near the base of the east slope of the median valley just north of the Vema F.Z. (dredge 3, figures 3 and 4).

These platy lava fragments may be pieces of single flows (Bonatti 1968), but are more likely crusts from which lava has been periodically withdrawn on the surface of a formerly active, churning lava lake. It is unlikely that single flows of any reasonable basalt viscosity could flow far from a vent in such thin flows without solidification. If these samples were from the surface of a lava lake, the lake was disrupted by faulting because the samples were collected on a sloping surface (figure 4). These platy basalts do not differ in composition from the normal pillow lavas in the region (table 3). DeBoer, Schilling & Krause (1969) have used such samples with recognizable tops and bottoms for magnetic vector orientation studies on the Reykjanes Ridge.

TABLE 4. SOME REPORTED OCCURRENCES OF 'XENOCRYSTS' FROM THE M.A.R.

locality	plagioclase composition	phases†	source	remarks	suggested origin
49° 50′ N	87–92 An	olivine ($Fo_{90.5}$), chromian spinel	Muir & Tilley (1964)	rounded, partially resorbed	xenocrysts from layered basic complex
45° 21′ N, 28° 2′ W; 45° 22′ N, 28° 13′ W	86 An	olivine (Fo_{86}), clinopyroxene (no composition given)	Aumento (1968)	rounded, partially resorbed	resorbed phenocrysts, in tially formed in volcar cupolas; resorption due increase in pressure du ing further ascent
30° 04′ N, 42° 16′ W; 29° 03′ N, 44° 16′ W	78–82 An	none	Muir & Tilley (1966)	rounded, partially resorbed	xenocrysts
28° 43′ N	bytownite	olivine (Fo_{90-95})	Nicholls *et al.* (1964)	phenocrysts	near surface crystallizati
23–25° N; 30° N	70–85 An	olivine (no composition given)	Miyashiro *et al.* (1969)	rounded, corroded, thin rim of more sodic composition	true phenocrysts since c cisive evidence for xen crystic origin is lacking
22° N	82–89 An	olivine (Fo_{85}), chromian spinel	Melson *et al.* (1968)	rounded, partially resorbed	resorbed phenocrysts: resorption due to pressu decrease at nearly co stant temperature
9–11° N‡	83–85 An	olivine (Fo_{85}), chromian spinel (rare)	this paper	rounded, partially resorbed; also large phenocrysts	cognate origin

† All these phases do not necessarily coexist in same specimen.
‡ See table 4 for localities where xenocrysts were observed.

Petrography

No strikingly unusual petrographic features were noted compared to already described M.A.R. basalts. Rounded, apparently resorbed, crystals of plagioclase and more rarely of olivine and chromite occur in trace amounts in most of the basalts, and in a few samples are abundant (figure 7, plate 4). In some samples they occur with large euhedral crystals. Most samples were greater than 90 % liquid at the time of extrusion. The bulk chemical analyses of two of the three analysed samples (table 2, analyses 2 and 3) reflect liquid compositions, whereas the other (analysis 1) reflects the presence of 10 % plagioclase phenocrysts.

The properties and origin of the rounded resorbed crystals, commonly referred to as xenocrysts, in M.A.R. basalts are of special interest. Such crystals have been noted by most petrologists who have worked on M.A.R. basalts (table 4). Those from the M.A.R. are the best

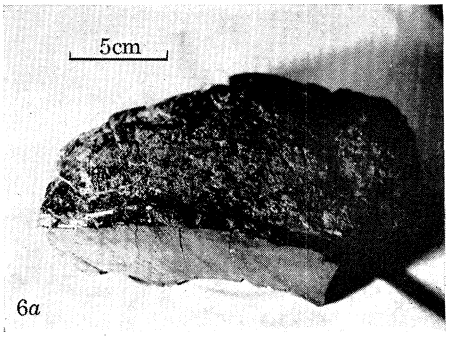

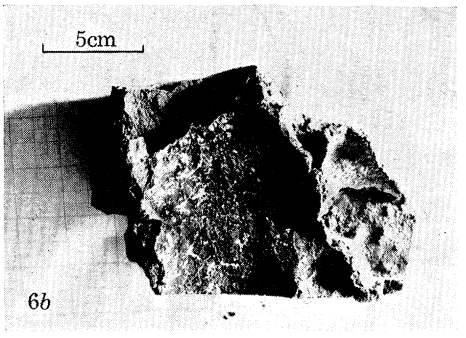

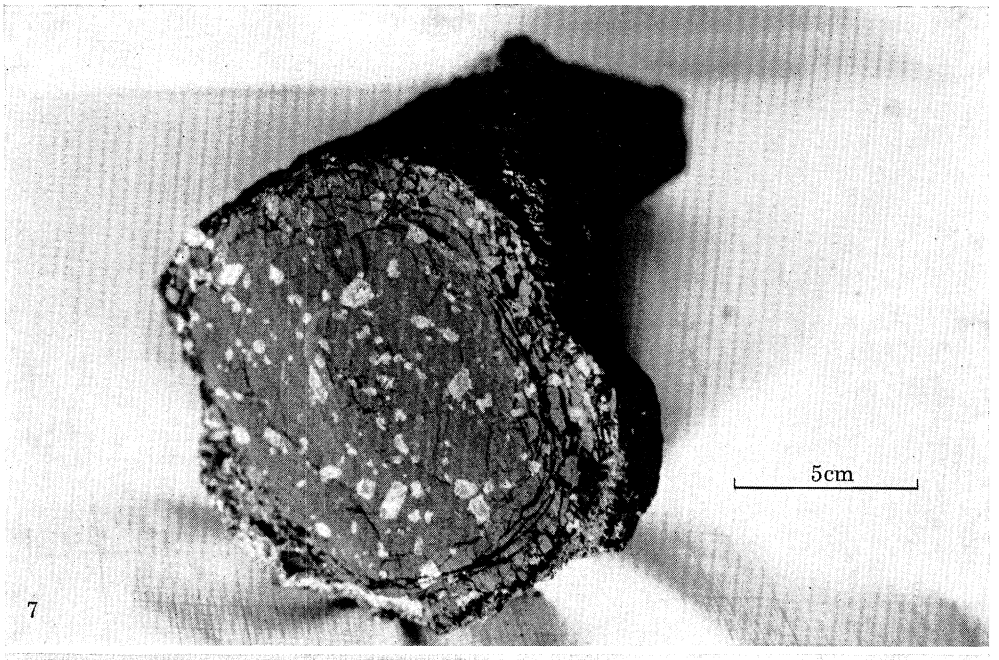

FIGURE 6. Platy lava fragment, quenched on two sides and having a convoluted, unpalagonitized presumably down-facing surface. (*a*) Top and side view; (*b*) Bottom view. Specimen about 18 cm in maximum dimension. Analysed sample (analysis 1, table 2).

FIGURE 7. Rounded and euhedral crystals of plagioclase, and very rarely of olivine, in a pillow basalt from the ridge segment south of the Vema F.Z. (dredge 58, figures 3 and 4, analysed sample, analysis 1, table 2).

FIGURE 8. Partially serpentinized plagioclase peridotite. White areas are weathered olivine; dark areas in matrix are mainly serpentine. Note infiltration of lighter coloured serpentine along bottom joint surface. Large oval, elongated bodies are enstatite porphyroclasts which have high alumina interiors. Sample is about 8 cm wide.

(*Facing p.* 430)

PHILOSOPHICAL TRANSACTIONS OF THE ROYAL SOCIETY A MATHEMATICAL, PHYSICAL & ENGINEERING SCIENCES

documented, but 'xenocrysts' have also been reported from other parts of the oceanic ridge system. Normally, very calcic plagioclase with lesser olivine are the main xenocrystal minerals. Traces of chromite occur, and clinopyroxene has been reported, although we believe the latter mineral to be extremely rare as a xenocrystal mineral in ocean ridge basalts. The plagioclase and olivine partially resorbed crystals have been considered as accidental inclusions of fragments of basic layered complexes (Muir & Tilley 1964). Other workers have favoured a cognate origin, involving an intermediate depth of crystallization followed by rapid essentially adiabatic rise causing resorption of the earlier formed phenocrysts (Aumento 1968; Melson *et al.* 1968).

TABLE 5. COMPOSITION† OF COEXISTING PLAGIOCLASES AND OLIVINES IN BASALTS FROM THE VEMA FRACTURE AREA

	plagioclase (An)						olivine (Fo)					
sample	1	2	3	4	5	6	1	2	3	4	5	6
AII–20–3–5	83	64	×	×	63	62	p	×	×	84	81	×
AII–20–58–27	84	×	84	74	×	62	p	×	×	×	85	×
AII–20–6–16	82	×	×	×	×	56	×	×	×	×	×	×
AII–20–6–17	85	69	×	×	×	65	×	×	×	×	×	×
AII–20–6–20	80	×	×	×	×	55	×	×	×	86	×	83
AII–20–6–25	×	×	70	68	69	63	×	×	×	84	×	×

† Composition given in percent anorthite molecule (An) and percent forsterite molecule (Fo). Analyses by electron probe.

1, large crystals with rounded shape (xenocrysts or resorbed phenocrysts); 2, very thin overgrowths on 1; 3, large phenocrysts (> 3 mm); 4, intermediate phenocrysts (< 3 mm, > 1 mm); 5, microphenocrysts (< 1 mm); 6, 'quench' groundmass microlites; p, present but not analysed; ×, not noted in thin section.

TABLE 6. RATIO OF AN CONTENT OF XENOCRYSTS TO NORMATIVE PLAGIOCLASE CONTENT OF MATRIX $-R_1$, AND TO NORMATIVE AN CONTENT OF MICROLITES $-R_2$

sample	R_1	R_2
AII–20–3–5	3.0	1.3
AII–20–58–27†	3.1	1.4
AII–20–6–16	2.8	1.5
AII–20–7–17	n.a.	1.3
AII–20–6–20	n.a.	1.5
AII–20–6–25‡	n.a.	1.1

† Corrected for about 10 % plagioclase xenocrysts. Xenocrysts compose less than 1 % of other two samples (AII–20–6–16 and AII–20–3–5).

‡ No xenocrysts present. Ratio is that of compositions of large plagioclase phenocrysts and microlites.

n.a. not analysed.

We have found an apparently systematic relationship between plagioclase xenocryst composition and the composition of coexisting quench crystals. The more calcic the xenocrysts, the more calcic the coexisting plagioclase microlites (table 5). Also, for the analysed samples, the ratio of xenocryst composition to the composition of normative plagioclase in the coexisting liquids is approximately constant (table 6). The total scatter of our data is, however, small and thus does not provide an optimal test for the presence or absence of systematic relationship between xenocryst and matrix compositions. Another feature of petrogenetic importance is the occurrence of glass inclusions in the plagioclase xenocrysts. Aumento (1968) has noted what he has identified as gas inclusions in plagioclase xenocrysts from 45° N latitude. We have found

PHILOSOPHICAL TRANSACTIONS OF THE ROYAL SOCIETY A MATHEMATICAL, PHYSICAL & ENGINEERING SCIENCES

glass inclusions with a small gas bubble, but from nowhere on the M.A.R. have we found solely gas inclusions in xenocrysts. The glass inclusions in one sample have the same composition as the glassy matrix in which they occur (xenocrysts in glassy rind of sample A1120–58–27, figure 7). This indicates that before resorption the plagioclase crystallized in the magma in which they now occur, and thus strongly supports a cognate origin for the xenocrysts.

The occurrence of phenocrysts and xenocrysts in the same sample is also noteworthy (figure 7). This feature we find difficult to explain, but it must involve mixing of crystals which have had quite different histories. In this particular sample, the largest phenocrysts and the xenocrysts have identical compositions (around An_{84}).

In the basalts described here the xenocrysts appear to have a cognate origin. This origin may involve either: (1) partial crystallization by cooling at an intermediate depth followed by rapid, adiabatic ascent causing resorption (i.e. resorption caused by decreasing pressure at constant temperature); or (2) partial crystallization in a near-surface magma chamber, followed by movement of crystals into deeper hotter portions of the magma chamber, with the movement perhaps aided by convection (i.e. resorption caused by increasing temperature at constant pressure). Of these two cognate origins, we believe the latter to be most likely.

There are significant differences in xenocryst composition from one locality to another along the M.A.R. (table 4). Thus, there may not be a single process which can account for all xenocrysts in these submarine basalts. A likely origin for xenocrysts at one locality can thus not be assumed to hold for all other localities.

Chemical characteristics

Basalts from the deep portions of the mid-ocean ridges differ systematically from continental and volcanic island basalts (Engel, Engel & Haven 1965). The basalts analysed here (table 3) show the chemical characteristics which are now so well documented for ocean-ridge basalts, such as low K_2O contents and normative compositions falling within the normative ternary system diopside–olivine–hypersthene. As the major and minor element concentrations, the trace element concentrations are quite like those of most deep-sea basalts (compare Engel *et al.* 1965; Melson *et al.* 1968; Aumento 1968, and average table 3). With the possible exception of strontium, no consequence of the abundance of plagioclase is noted on the trace element concentrations in sample 1 (table 3). Typically, as for the basalts in hand, deep-sea basalts contain normative olivine, and only rarely contain either normative quartz or normative nepheline. If examined more closely, analyses of deep-sea basalts do show systematic compositional variations. Large numbers of analyses from a single dredge and nearby dredges may show distinctive linear trends or groupings on plots of total iron as FeO/MgO against Al_2O_3 and MgO (Miyashiro *et al.* 1969*a*, p. 50). On the basis of such plots, low alumina, high MgO basalts (low alumina abyssal tholeiites) and high alumina, low MgO basalts (high alumina abyssal tholeiites) have been distinguished. On the basis of this classification, samples 2 and 3 (table 3) are 'low-alumina abyssal tholeiites' (fig. 3 of Miyashiro *et al.* 1969*a*). Sample 1 (table 3) falls into the high-alumina abyssal basalt field, but this is a direct consequence of the abundance of plagioclase xenocrysts and phenocrysts. Thus, there is no evidence in our basalts for the existence of high-alumina basaltic liquids.

PHILOSOPHICAL TRANSACTIONS OF THE ROYAL SOCIETY A MATHEMATICAL, PHYSICAL & ENGINEERING SCIENCES

Ultramafic rocks

Macroscopic features

Partially serpentinized peridotites were the main rock type at station 9 and small pebbles of ultramafic rocks were found at station 59 (figures 3, 4). The latter samples have not been examined in as great detail. The collection from station 9, which is near the base of the south wall of the fracture zone, is homogeneous and consists of partially weathered and serpentinized plagioclase chromite peridotite. The samples have tectonic features and show well-developed banding (figure 8, plate 4). The banding is a result of shearing out of an originally coarse-grained peridotite. Large augen of enstatite remain, but most other primary minerals occur as either very small augen or as recrystallized matrix granules. Contrasts in the alumina content between the large enstatite augen and enstatite matrix granules show that chemical adjustments accompanied the mechanical deformation. Serpentinization is nearly complete near joint surfaces which bound the samples and along veinlets which penetrate the sample. Away from these, the relicts of most primary minerals are abundant. A single sample was selected for chemical and modal analysis (table 7). The modal analysis is only approximate ($\pm 10\,\%$). Each band appears to differ slightly from each other band and thus modal analyses on a single thin section may not be representative of the whole sample.

Table 7. Composition and mode of partially serpentinized peridotite
(USNM 111339; original number A II–20–9–1)

		trace elements (parts/10)[6]		mode (approximate) (volume %)	
SiO_2	39.71				
Al_2O_3	2.59	B	70	Primary minerals	
Fe_2O_3	7.31	Ba	5	olivine	7
FeO	1.30	—	—	orthopyroxene	5
MgO	33.15	Cr	3300	clinopyroxene	1
CaO	1.52	Cu	18	plagioclase	1
Na_2O	0.28	Ga	10	chromian spinel	1
K_2O	0.06	Li	13		
H_2O^+	11.29	Ni	2300	Secondary minerals	
H_2O^-	1.59	Pb	22	serpentine	60
TiO_2	0.06	Sr	10	orange-brown mineral after olivine (submarine weathering product)	20
P_2O_5	0.02	V	110		
MnO	0.12	Y	8	magnetite (?)	4
NiO	0.27	Zn	50		
Cr_2O_3	0.44	Zr	< 5		
total	99.71				

E. Jarosewich, analyst for major and minor elements. G. Thompson, analyst for trace elements.
The following trace elements were also sought but if present were below their detection limit (ppm): Ag (< 1), Bi, Cd (< 2); Mo, Sn, (< 5); Rb (< 20).

Petrography

Emphasis in the examination of these samples has been placed on the primary, high temperature phases. We have no data on the minerals produced during serpentinization or weathering. The primary phases compose about 15 % by volume of the samples. They typically occur as augen or in schlieren, and have thus undergone shearing and recrystallization, presumably during upward movement and emplacement in the oceanic crust. Olivine (*ca.* Fo_{90}) is the most abundant primary mineral and occurs as minute matrix granules in pools of serpentine minerals.

Orthopyroxene (enstatite, *ca.* En_{90}, table 8) is the second most abundant primary mineral, and occurs as conspicuous large augen (figure 8) with a small percentage of exsolved clinopyroxene lamella. The margins of the augen are sheared, and the matrix contains abundant enstatite granules derived from the shearing out of the larger crystals. The enstatite augen have high alumina cores which are surrounded by a thin outer zone of low alumina content. The outer zones have low alumina contents that are comparable to the matrix enstatite granules (figure 9). The alumina content of the interior of the augen are similar to the high alumina contents noted in enstatite augen from the Tinaquillo and Lizard complexes and somewhat higher than those of the St Paul's Rocks peridotite. A comparison and data sources are shown in figure 9.

TABLE 8. IRON, CALCIUM AND MAGNESIUM CONTENTS OF COEXISTING GRAINS OF CLINOPYROXENE (COLUMNS 1 TO 7) AND ORTHOPYROXENE (COLUMNS 8 TO 12).† AMOUNT OF WOLLASTONITE (Wo), ENSTATITE (En), AND FERROSILITE (Fs) MOLECULES CALCULATED ASSUMING ALL Fe IN FERROSILITE MOLECULE. SAMPLE OF PARTIALLY SERPENTINIZED PLAGIOCLASE CHROMITE PERIDOTITE, DREDGE 9, VEMA F.Z. (A II–20–9–1).

	1	2	3	4	5	6	7	8	9	10	11	12
Fe	2.9	2.4	2.4	2.3	2.7	2.4	1.9	5.4	5.3	5.5	5.1	5.2
CaO	12.7	14.8	15.0	15.5	13.7	14.9	14.9	0.8	0.5	0.9	1.6	1.4
MgO	10.4	9.2	9.2	9.1	10.4	10.4	10.2	20.0	20.2	20.9	19.1	19.5
Wo	40	47	47	48	42	44	45	2	1	2	4	4
En	54	48	48	47	52	51	51	88	89	88	86	86
Fs	6	5	5	5	6	5	4	10	10	10	10	10
X_{Mg}‡	0.91	0.90	0.90	0.90	0.90	0.91	0.92	0.90	0.90	0.90	0.90	0.90

† Accuracy: maximum error around ±10% amount present.
‡ X_{Mg} = molar ratio Mg/Mg+Fe.

Clinopyroxene (*ca.* $En_{50}Wo_{45}Fs_5$, table 8) occurs as small recrystallized grains which are abundant in certain bands. Individual large augen of clinopyroxene were not noted in the three thin sections studied in detail. If clinopyroxene augen are present, they probably compose less than 10% of the augen population. The compositional spread of Ca, Mg, and Fe contents in various coexisting ortho- and clinopyroxenes in these and other samples of ultramafic rocks from the M.A.R. is quite small (figure 10). Most of the clinopyroxenes fall in the diopside-endiopside fields. Minor elements in the clinopyroxenes from the Vema F.Z. peridotite (sample 9–1) include Al_2O_3 (1.3%), TiO_2 (0.3%), and Na_2O (0.3%). Table 8 gives electron probe analyses for Fe, Ca, and Mg for various grains of the pyroxenes in this sample.

Plagioclase (*ca.* An_{73}) occurs as small isolated matrix granules, which probably composed around 1 to 5% of the original unaltered sample. The plagioclase is surprisingly sodic for an ultramafic rock, and thus its composition was double-checked. Examination of a plagioclase peridotite from the Romanche Trench (sample A1120–23–7, Woods Hole Oceanographic Institution) gave a plagioclase composition which averages around An_{70}. It thus appears that this composition may not be atypical for plagioclase from peridotites in Equatorial Atlantic fracture zones.

Brown presumably chromian spinel occurs as rare augen and matrix granules. No electron probe analyses were obtained on this mineral.

PHILOSOPHICAL TRANSACTIONS OF THE ROYAL SOCIETY A MATHEMATICAL, PHYSICAL & ENGINEERING SCIENCES

Chemical characteristics

Alteration by serpentinization followed by submarine weathering has caused drastic changes in the primary composition of the peridotites (table 7). Particularly noteworthy secondary effects include the very high-water content and high Fe_2O_3/FeO ratio. Among the trace elements, enrichment in boron is particularly significant. This feature may be either attributed to addition of boron from sea water during weathering or from the hydrothermal solutions which caused serpentinization. Other compositional changes (e.g. increase in lithium and barium concentration) that normally accompany sea-water weathering are not noted. Boron enrichment is well

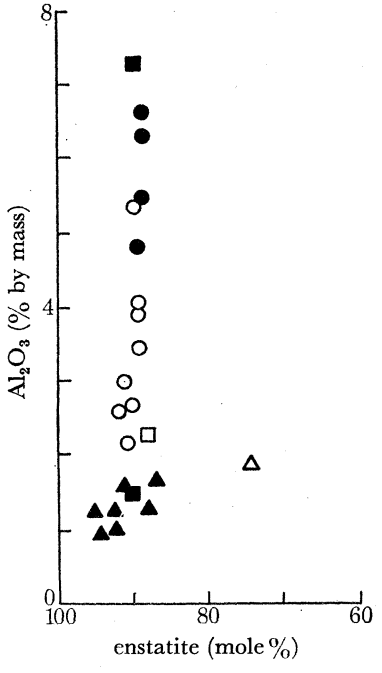

FIGURE 9

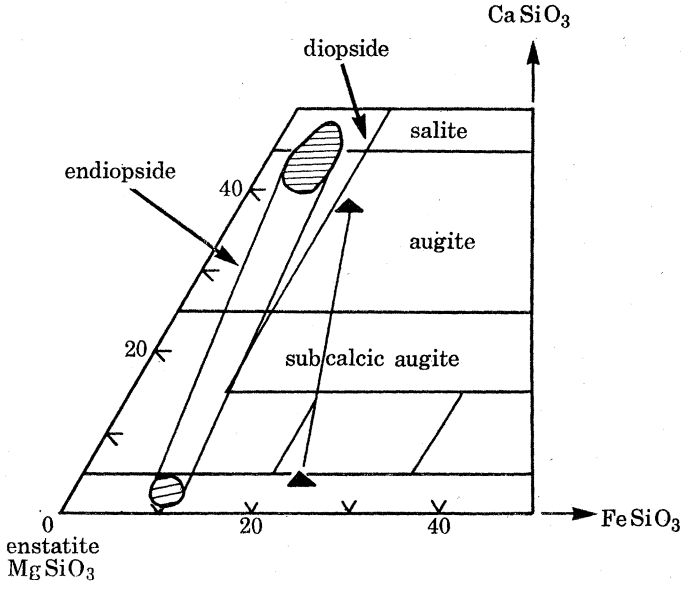

FIGURE 10

FIGURE 9. Alumina content of centre of an enstatite augen and of recrystallized enstatite matrix granules and augen margin (sample A II–20–9–1, serpentinized plagioclase peridotite, Vema F.Z.). The orthopyroxene and the laminated gabbro from the Romanche fracture have been described by Melson & Thompson (1970). Other data are from Green (1964). ■, peridotite (Vema F.Z.); □, peridotite (Romanche fracture); ●, Lizard peridotite; ○, peridotite nodules; ▲, other continental peridotite intrusions; △, laminated gabbro (Romanche fracture).

FIGURE 10. Compositional spread of coexisting pyroxenes in serpentinized peridotites from the Vema F.Z. (sample A II–20–9–1) and Romanche fracture (sample A II–20–23–7). The stippled field includes coexisting pyroxenes in a very coarse-grained gabbro from 4° S, M.A.R. (sample A II–42–2–6, Woods Hole Oceanographic Institution, see Thompson *et al.* 1969). Also included for comparison are coexisting pyroxenes from a gabbro with cumulate texture from the Romanche fracture (sample A II–20–16–46, Melson & Thompson, 1970).

documented for many continental serpentinites, and is evident in another deep-sea serpentinized peridotite from the Indian Ocean (Engel & Fisher 1969, sample 93–3, table 3). The implications of the boron contents of various deep-sea igneous and metamorphic rocks has been discussed elsewhere, and ultimate derivation of the boron from mantle-derived hydrothermal solutions rather than from sea water is favoured (Thompson & Melson 1970).

The analysed sample (table 7, sample A II–20–9–1) was analysed for rare earth abundances by F. Frey. He reports (personal communication) that the heavy rare earths (Tb–Lu) have

chondritic abundances, whereas the light rare earth elements are increasingly depleted from Tb to La. The overall distribution is similar to ridge basalts, although ridge basalts are enriched by more than a factor of 20 in absolute rare earth element abundances.

Petrogenesis

The relationship between deep sea peridotites and ocean ridge basalts, and the P–T conditions under which the peridotites crystallized are major petrologic problems. The data on the peridotite presented here bears on these problems but allows no general conclusions.

The partioning of Mg and Fe between coexisting orthopyroxene and clinopyroxene is a function of the pressure and temperature at which the pyroxenes equilibrated. Temperature has been shown to influence the distribution more importantly than pressure (Kretz 1961, 1963). The distribution coefficient, K_d, is defined by

$$K_d = \frac{X^o_{Mg}(1 - X^c_{Mg})}{X^c_{Mg}(1 - X^o_{Mg})},$$

where X^o_{Mg} = the mole fraction of Mg in the orthopyroxene and X^c_{Mg} = the mole fraction of Mg in the clinopyroxene (mole fraction in molar amount Mg/Mg + Fe in each pyroxene). K_d is typically smaller for basic granulites than it is for basic igneous rocks, a difference believed to be due primarily to the higher temperature of the latter (Kretz 1961). For example, K_d for basic granulites is typically around 0.53, and 0.73 for gabbros (Kretz 1961, p. 373).

The data for coexisting pyroxenes in the Vema F.Z. sample (table 8), although not of high accuracy, permit calculation of an approximate value of K_d. K_d appears to be very close to one. For the maximum difference between X^c_{Mg} and X^o_{Mg} (0.92 and 0.09, respectively), a minimum value of 0.78 is obtained. The more likely value for K_d is around 1.0 and is higher than the K_d of gabbros and much higher than the K_d of basic granulites. This raises the possibility that these periodotites equilibrated at temperatures in excess of the crystallization temperatures of most gabbroic pyroxenes, temperatures which are typically between 1000 and 1200 °C. On plots of X^c_{Mg} against X^o_{Mg} (Kretz 1961, fig. 7), the average values for the Vema F.Z. sample fall within the cluster of values for coexisting pyroxenes in olivine nodules from basalts (Ross, Foster & Myers 1954).

A more elaborate scheme to derive temperatures and pressures of crystallization for coexisting pyroxenes has been put forth by O'Hara (1967). However, the pyroxenes in the Vema F.Z. peridotite crystallized under different conditions as shown by the variation in alumina content of the enstatite. This may be why we failed to be able to use O'Hara's scheme. A similar variation was not found in the Fe/Fe + Mg ratios of the pyroxenes, suggesting that conditions changed so as to give variations in Al content without variations or with but small variation in Fe/Fe + Mg ratio. If alumina substitution within the plagioclase peridotite stability field is a function mainly of pressure rather than temperature (Green 1963), the variation in enstatite alumina contents may be taken to reflect ascent into the crust at essentially constant temperature, and with but partial equilibrium of the enstatite.

The approximate stability fields of various peridotite assemblages have been outlined by Green & Ringwood (1967) as well as by a number of other authors. The Vema F.Z. primary assemblage belongs within the plagioclase pyrolite stability field (figure 11). For an assumed equilibrium temperature of around 1200 °C, an upper limit of burial of 30 km is obtained. At

pressures in excess of those at this depth (*ca.* 10 kbar; 1 MN m^{-2}), plagioclase would no longer be a stable phase. The reaction involved along this field boundary is of the type

$$(MgAl_2O_4 + FeCr_2O_4) + CaMgSi_2O_6 + 2MgSiO_3 = CaAl_2Si_2O_8 + 2Mg_2SiO_4 + FeCr_2O_4$$
spinel ss diopside enstatite anorthite olivine chromite

This reaction, because of the possible variations of Fe/Mg ratios and of Na and Al contents of some of the phases, is not univariant, but rather takes place over a range of temperatures and pressures. Thus the boundary between the stability fields of the plagioclase and spinel peridotites which is shown as a line in figure 10, may be viewed more correctly as a zone of as yet undefined width and one whose width will differ for samples of different bulk compositions.

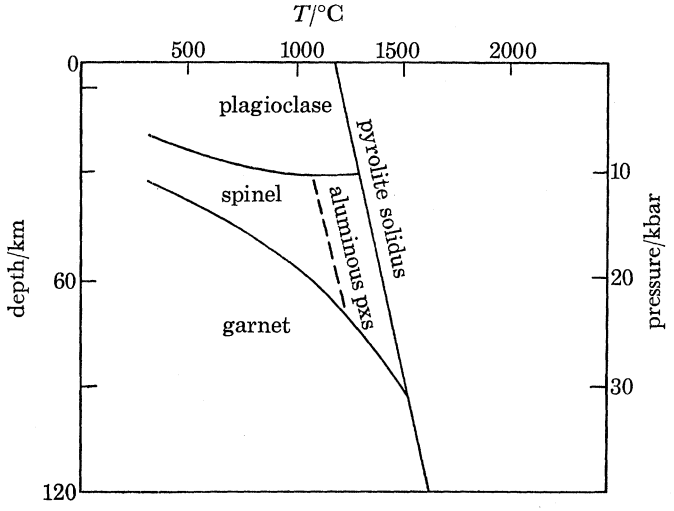

FIGURE 11. Stability fields of various peridotite (pyrolite) assemblages (modified from Green & Ringwood 1967). The Vema F.Z. samples have equilibrated within the plagioclase pyrolite stability field. Olivine, orthopyroxene and clinopyroxene are stable in all fields.

The properties, classification, and origin of ultramafic rocks have recently been extensively reviewed (Wyllie 1967). Postulated relations between peridotites and basaltic magma include: (1) peridotites in some cases are the residua after extraction of basaltic liquids (figure 12), (2) some peridotites are cumulates formed by settling of mainly olivine crystals from slowly crystallizing basaltic magma in large crustal or upper mantle magma chambers, and (3) some peridotites are undifferentiated mantle material. Criteria for the recognition of these possible genetic types are not clear-cut. Certain textural features, such as chromite layers (Thayer 1969), point to a cumulate origin. Chemical and mineralogical criteria are not well established, and even textural criteria (e.g. cumulate textures) become obscured by extensive shearing in many peridotites, as in the case of the peridotites from St Paul's Rocks (Melson *et al.* 1967*a*). The Vema F.Z. peridotite textures and mineralogy are similar to the peridotite mylonite at St Paul's Rocks except that the latter are much finer grained. We have not found sheared gabbroic rocks in the Vema F.Z. like those that occur in association with the peridotites at St Paul's Rocks (Melson *et al.* 1967*a*, *b*), nor layered and fractionated gabbros like those that occur in large basic intrusions in the oceanic crust as in the Romanche fracture (Melson & Thompson 1970). The data presented here appear to be compatible with the view that the Vema F.Z. peridotites may be close to undifferentiated mantle material. The rare earth element concentrations and the

moderately high alkali and titanium contents (table 7) would appear in accord with this view. However, the sample has undergone extensive alteration and these compositional features may reflect the alterations rather than the primary composition. A possible model for emplacement of undifferentiated mantle in the crust may be illustrated by reference to figure 12. An upward moving diapir (subsolidus) either cooled sufficiently during its ascent that it did not intersect the solidus, or it intersected the solidus but the resulting liquid and crystals did not separate, but were rather emplaced in the crust as a crystal mush.

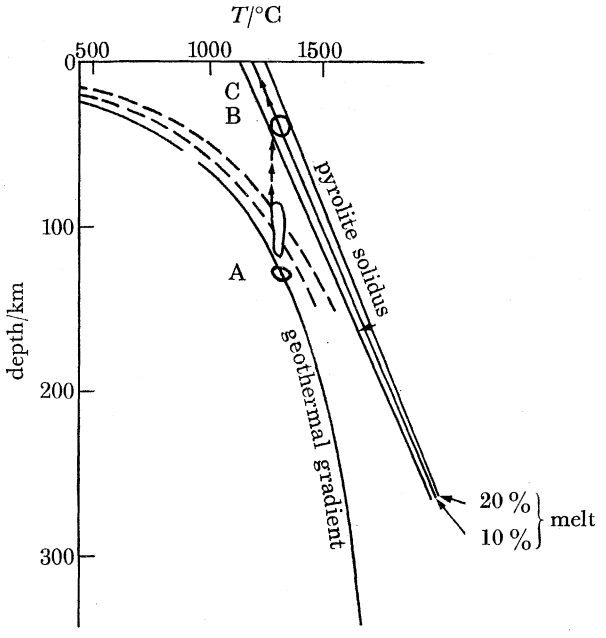

FIGURE 12. A model for magma formation by fractional melting of mantle pyrolite (simplified from Green & Ringwood 1967). Thermal instability leads to the diapiric ascent of bodies of subsolidus pyrolite. These rise at essentially constant temperature until they intersect the pyrolite solidus and begin to melt. Beyond the solidus the bodies ascend as crystal mushes until magma and residual crystals become separated. The extent of melting before separation of crystals and liquid and the point at which the diapirs intersect the solidus largely control magma composition.

The peridotites from the Romanche fracture appear to have much higher $^{87}Sr/^{86}Sr$ ratios than those of ocean-ridge basalts (Bonatti, this volume, p. 385). This is not readily attributable to sea-floor weathering effects, and high $^{87}Sr/^{86}Sr$ ratios have been observed in certain continental peridotites (Hurley 1967). Eight continental dunites were reported by Hurley (1967) to have a mean $^{87}Sr/^{86}Sr$ ratio of 0.712, whereas the peridotites of St Paul's Rocks have a mean ratio of 0.704, similar to oceanic basalts. If this high $^{87}Sr/^{86}Sr$ is a feature of the primary peridotites, it is most difficult to explain in terms of any of the just mentioned possible relationships between oceanic basalts and oceanic peridotites. The boron enrichment we found shows that major trace element changes do accompany alterations of deep-sea peridotites. If these alterations also involve additions of Sr that is highly enriched in radiogenic strontium (^{87}Sr) a high $^{87}Sr/^{86}Sr$ ratio would result. Interaction with sea water would raise the $^{87}Sr/^{86}Sr$ somewhat, but not as high as some of the reported values for the Romanche fracture (Bonatti, this volume).

Summary and conclusions

(1) A marked contrast exists between the rocks of the transform fault (Vema F.Z.) and the adjacent ridge segments. Along the ridge axes, basaltic extrusions and intrusions accompany sea-floor spreading and give rise to a basaltic upper zone (layer 2). In the fracture zone, the upper basaltic zone has been rifted apart by a change in spreading direction (van Andel *et al.* 1969) exposing a predominantly serpentinite zone (layer 3?) capped in at least one region (DC–2, dredge 59, figures 3 and 4) by basaltic rocks.

(2) The basalts from both offset ridge segments have similar chemical and petrographic features, and are typical of deep-sea basalts from the mid-ocean ridges.

(3) Xenocrysts (rounded, partially resorbed crystals) of plagioclase and olivine, and much less commonly of chromite, occur in small amounts in most basalts and rarely compose up to 10 % by volume. These have a cognate origin and are believed to form by cooling and convection in near surface magma chambers.

(4) Serpentinized plagioclase peridotites from the fracture zone contain high-alumina enstatites. Their chemical and mineralogical features suggest (*a*) an originally high temperature (*ca.* 1200 °C), moderate pressure (< 10 kbar; 1 MN m^{-2}) equilibrium, followed by essentially adiabatic emplacement either as a crystal mush or subsolidus plastic mass into the oceanic lower crust (layer 3), and (*b*) that the primary peridotites described here may be chemically unfractionated upper mantle. This latter conclusion should not be applied to all oceanic peridotites; others have distinctly different properties and origins.

(5) Equatorial Atlantic transform fault zones and those of the Indian Ocean appear to expose layer 3, which appears to be a complex of plutonic and metamorphic rocks in which peridotites predominate with subordinate gabbro, greenschist metabasite, amphibolite and other rock types. The peridotites of fracture zones mainly equilibrated in the plagioclase pyrolite facies before their emplacement in oceanic crust. Some fracture zones, such as most of those of the eastern Pacific, are, or have been, the sites of basaltic eruptions, which tend to cover deeper exposures given by faulting and may even build ridges (e.g. the Mendocino Ridge).

The samples studied were collected on cruise 20 of R.V. *Atlantis II*, Woods Hole Oceanographic Institution; Dr V. T. Bowen was chief scientist. We thank the officers, crew and scientists on board R.V. *Atlantis II* for their assistance. We also thank Professor Tj. H. van Andel (Oregon State University) for use of bathymetric diagrams and Dr V. T. Bowen for criticism of the original manuscript; both Dr Bowen and Professor van Andel were instrumental in starting the overall studies of the Vema fracture region. This work was completed with the aid of Smithsonian research grants and the U.S. Atomic Energy Commission under contract AT(30–1)–2174 with the Woods Hole Oceanographic Institution. This support is gratefully acknowledged.

This is contribution no. 2503 from the Woods Hole Oceanographic Institution.

PHILOSOPHICAL TRANSACTIONS OF THE ROYAL SOCIETY A MATHEMATICAL, PHYSICAL & ENGINEERING SCIENCES

References (Melson & Thompson)

Aumento, F. 1968 The Mid-Atlantic Ridge near 45° N. II. Basalts from the area of Confederation Peak. *Can. J. Earth Sci.* **5**, 1–21.

Bogdanov, Yu. A. & Ploshko, V. V. 1968 Igneous and metamorphic rocks from the abyssal Romanche Depression. *Dokl. Akad. Nauk SSSR* **177**, 173–176.

Bonatti, E. 1968 Fissure basalts and ocean-floor spreading on the East Pacific Rise. *Science, N.Y.* **161**, 886–888.

Bonatti, E. 1968 Ultramafic rocks from the Mid-Atlantic Ridge. *Nature, Lond.* **219**, 363–364.

Bonatti, R. 1971 Ultramafic rocks from the Mid-Atlantic Ridge. *Phil. Trans. Roy. Soc. Lond.* A, this volume, p. 385.

Cann, J. R. 1968 Geological processes at mid-ocean ridge crests. *Geophys. J. R. astr. Soc.* **15**, 331–341.

Cann, J. R. 1969 Spilites from the Carlsberg Ridge, Indian Ocean. *J. Petrology* **10**, 1–19.

Cann, J. R. & Vine, F. J. 1966 An area on the crest of the Carlsberg Ridge: petrology and magnetic survey. *Phil. Trans. Roy. Soc. Lond.* A **259**, 198–217.

DeBoer, G., Schilling, J. G. & Krause, D. C. 1969 Magnetic polarity of pillow basalts from Reykjanes Ridge. *Science, N.Y.* **166**, 996–998.

Engel, A. E. J., Engel, C. & Haven, R. G. 1965 Chemical characteristics of oceanic basalt and the upper mantle. *Bull. geol. Soc. Am.* **76**, 719–734.

Engel, C. G. & Fisher, R. L. 1969 Lherzolite, anorthosite, gabbro and basalt dredged from the mid-Indian Ocean Ridge. *Science, N.Y.* **166**, 1136–1141.

Green, D. H. 1963 Alumina content of enstatite in a Venezuelan high-temperature peridotite. *Bull. geol. Soc. Am.* **74**, 1397–1402.

Green, D. H. 1964 The petrogenesis of the high-temperature peridotite in the Lizard area, Cornwall. *J. Petrology* **5**, 134–188.

Green, D. H. & Ringwood, A. E. 1967 Genesis of Basaltic Magmas. *Contr. miner. Petrol.* **15**, 103–190.

Hekinian, R. 1968 Rocks from the mid-oceanic ridge in the Indian Ocean. *Deep Sea Res.* **15**, 195–213.

Hess, H. H. 1962 History of ocean basins. In *Petrologic Studies* (Buddington volume) (ed. A. E. J. Engel, H. L. James & B. F. Leonard), pp. 599–620. Geological Society of America.

Hess, H. H. 1965 Mid-Oceanic ridges and tectonics of the sea floor. Colston Papers **17**, 317–332. London: Butterworths Scientific Publications.

Hurley, P. M. 1967 Rb^{87}, Sr^{87} relationships in differentiation of the mantle. *Ultramafic and related rocks* (ed. P. J. Wyllie), pp. 372–375. New York: Wiley and Sons.

Kretz, R. 1961 Some applications of thermodynamics to coexisting minerals of variable composition. Examples: orthopyroxene-clinopyroxene and orthopyroxene-garnet. *J. Geol.* **69** (4), 361–387.

Kretz, R. 1963 Distribution of magnesium and iron between orthopyroxene in natural mineral assemblages. *J. Geol.* **71**, 773–785.

Melson, W. G. 1968 Petrologic model of the earth's crust across the mid-Atlantic ridge. *Trans. Am. Geophys. Union* **49**, 364 (abstract).

Melson, W. G. 1970 Geophysical survey of the Juan de Fuca Ridge and Blanco Trough. *U.S.C. and G.S. Tech. Mem.* **3**, 30 pp.

Melson, W. G., Jarosewich, E., Bowen, V. T. & Thompson, G. 1967*a* St Peter and St Paul Rocks: a high temperature mantle derived intrusion. *Science, N.Y.* **155**, 1532–1535.

Melson, W. G., Jarosewich, E., Cifelli R. & Thompson, G. 1967*b* Alkali olivine basalt dredged near St Peter and St Paul's Rocks. *Nature, Lond.* **215**, 381–382.

Melson, W. G., Thompson, G. & van Andel, Tj. H. 1968 Volcanism and metamorphism in the mid-Atlantic Ridge, 22° N. latitude. *J. geophys. Res.* **73**, 5925–5941.

Melson, W. G. & Thompson, G. 1970 Layered basic intrusion in oceanic crust, Romanche Fracture, equatorial Atlantic. *Science, N.Y.* **168**, 817–820.

Miyashiro, A., Shido, F. & Ewing, M. 1969*a* Diversity and origin of abyssal tholeiite from the mid-Atlantic Ridge near 24° and 30° North latitude. *Contr. miner. Petrol.* **23**, 38–52.

Miyashiro, A., Shido, F. & Ewing, M. 1969*b* Composition and origin of serpentinites from the the mid-Atlantic Ridge near 24° and 30° N. latitude. *Contr. miner. Petrol.* **23**, 117–127.

Miyashiro, A., Shido, F. & Ewing, M. 1970 Petrologic models for the mid-Atlantic Ridge. *Deep Sea Res.* **17**, 109–123.

Miyashiro, A., Shido, F. & Ewing, M. 1971 Metamorphism in the mid-Atlantic Ridge near 24° and 30° N. *Phil. Trans. Roy. Soc. Lond.* A, this volume, p. 589.

Muir, I. D. & Tilley, C. E. 1964 Basalts from the northern part of the rift zone of the mid-Atlantic Ridge. *J. Petrology* **5**, 409–434.

Muir, I. D. & Tilley, C. E. 1966 Basalts from the northern part of the mid-Atlantic Ridge. II. The Atlantis collection near 30° N. *J. Petrology* **7**, 193–201.

Nicholls, G. D., Nalwalk, A. J. & Hays, E. E. 1964 The nature and composition of rock samples dredged from the mid-Atlantic Ridge between 22° N and 52° N. *Mar. Geol.* **1**, 333–343.

O'Hara, M. 1967 Mineral parageneses in ultrabasic rocks. In *Ultramafic and related rocks* (ed. P. J. Wylie), p. 393–403. New York: Wiley and Sons.

PHILOSOPHICAL TRANSACTIONS OF THE ROYAL SOCIETY A MATHEMATICAL, PHYSICAL & ENGINEERING SCIENCES

Phillips, J. D., Thompson, G., Von Herzen, R. P. & Bowen, V. T. 1969 Mid-Atlantic Ridge near 43° N latitude. *J. Geophys. Res.* **74**, 3069–3081.

Ploshko, V. V. & Bogdanov, Y. A. 1968 Ciperbazity glubokovodnoy vladiny romansch. *Izv. An SSSR* (ser. geol.) **12**, 82–93. English translation. *Int. Geol. Rev.* **11** (8), 902–910.

Ross, C. S., Foster, M. D. & Myers, A. T. 1954 Origin of dunites and of olivine-rich inclusions in basaltic rocks. *Am. Miner.* **39**, 693–737.

Sykes, L. R. 1967 Mechanism of earthquakes and nature of faulting on mid-oceanic ridges. *J. Geophys. Res.* **72**, 2131–2153.

Thayer, T. P. 1969 Alpine-type sensu strictu (ophiolitic) peridotites: refractory residues from partial melting of igneous sediments? A contribution to the discussion of the paper: 'Origin of ultramafic and ultrabasic rocks' by P. J. Wyllie. *Tectonophysics* **7**, 511–516.

Thompson, G., Melson, W. G. & Bowen, V. T. 1969 The mid-Atlantic Ridge at 4° S and implications concerning the petrology of the oceanic crust at mid-ocean ridges. *Trans. Am. Geophys. Union* **50**, 211.

Thompson, G. & Bankston, D. C. 1969 A technique for trace element analysis of powdered materials using the d. c. arc and photoelectric spectrometry. *Spectrochim. Acta* **24**B, 335–350.

Thompson, G. & Melson, W. G. 1970 Boron contents of serpentinites and metabasalts in oceanic crust: implications for the boron cycle in the oceans. *Earth Planet. Sci. Lett.* **8**, 61–65.

van Andel, Tj. H., Corliss, J. B. & Bowen, V. T. 1967 The intersection between the mid-Atlantic Ridge and the Vema Fracture Zone in the North Atlantic. *J. Marine Res.* **25**, 343–351.

van Andel, Tj. H., Phillips, J. D. & Von Herzen, R. P. 1969 Rifting origin for the Vema Fracture in the North Atlantic. *Earth Planet. Sci. Lett.* **5**, 296–300.

van Andel, Tj. H. 1969 Recent uplift of the mid-Atlantic Ridge south of the Vema Fracture Zone. *Earth Planet. Sci. Lett.* **7**, 228–230.

Vine, F. T. & Hess, H. H. 1970 Sea-floor spreading. *The seas*, vol. 4 (ed. A. Maxwell). New York: Interscience.

Wyllie, P. J. 1967 *Ultramafic and related rocks* (ed. P. J. Wyllie). New York: Wiley and Sons.

PHILOSOPHICAL TRANSACTIONS OF THE ROYAL SOCIETY A MATHEMATICAL, PHYSICAL & ENGINEERING SCIENCES

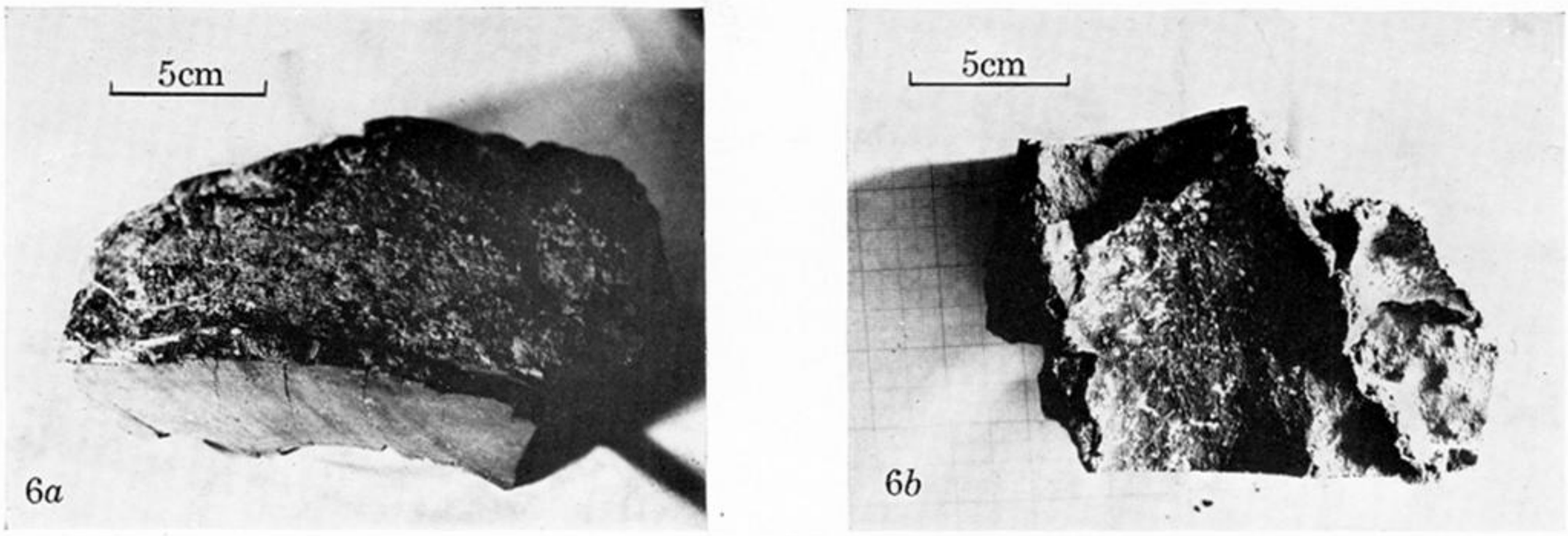

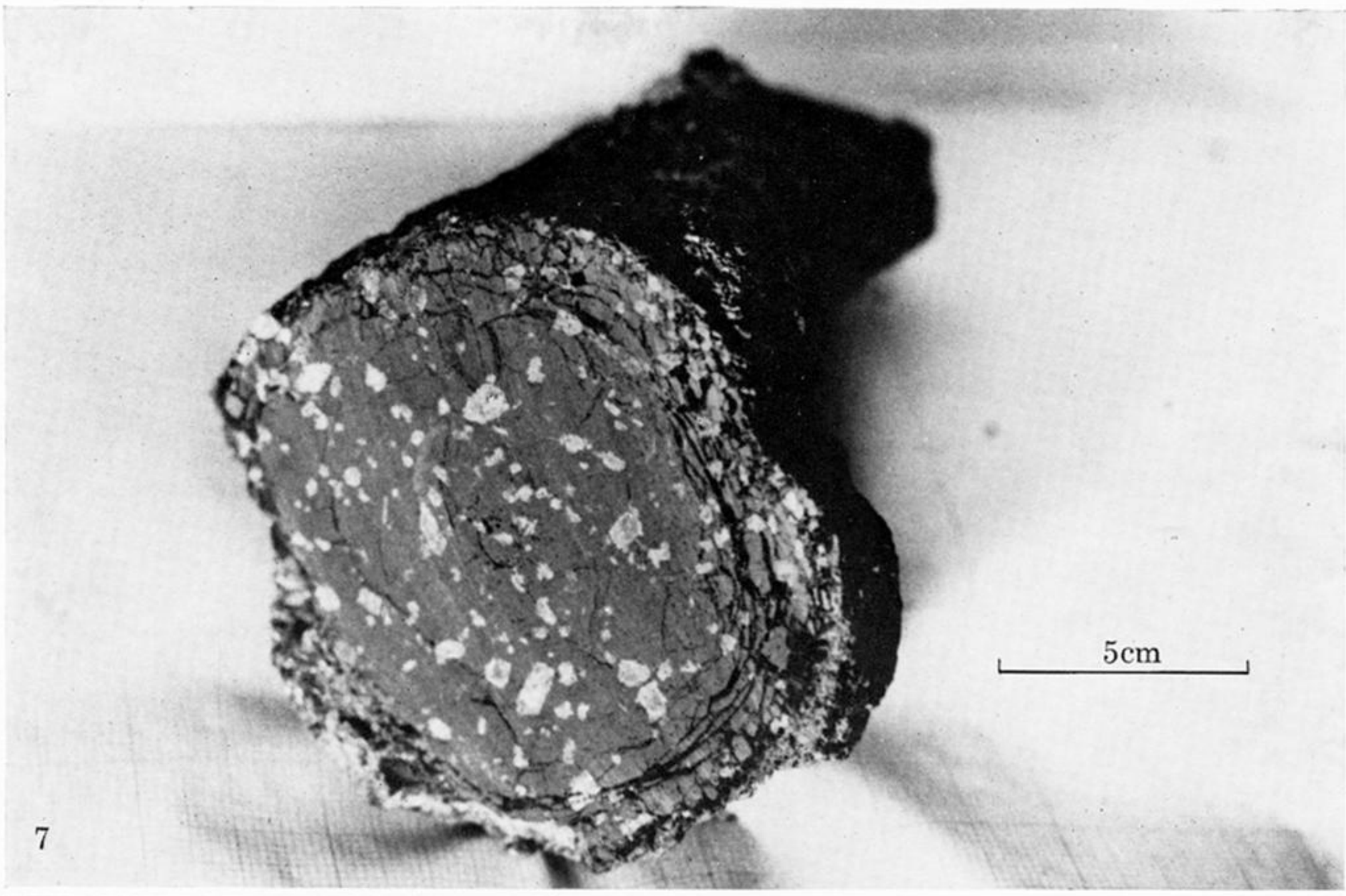

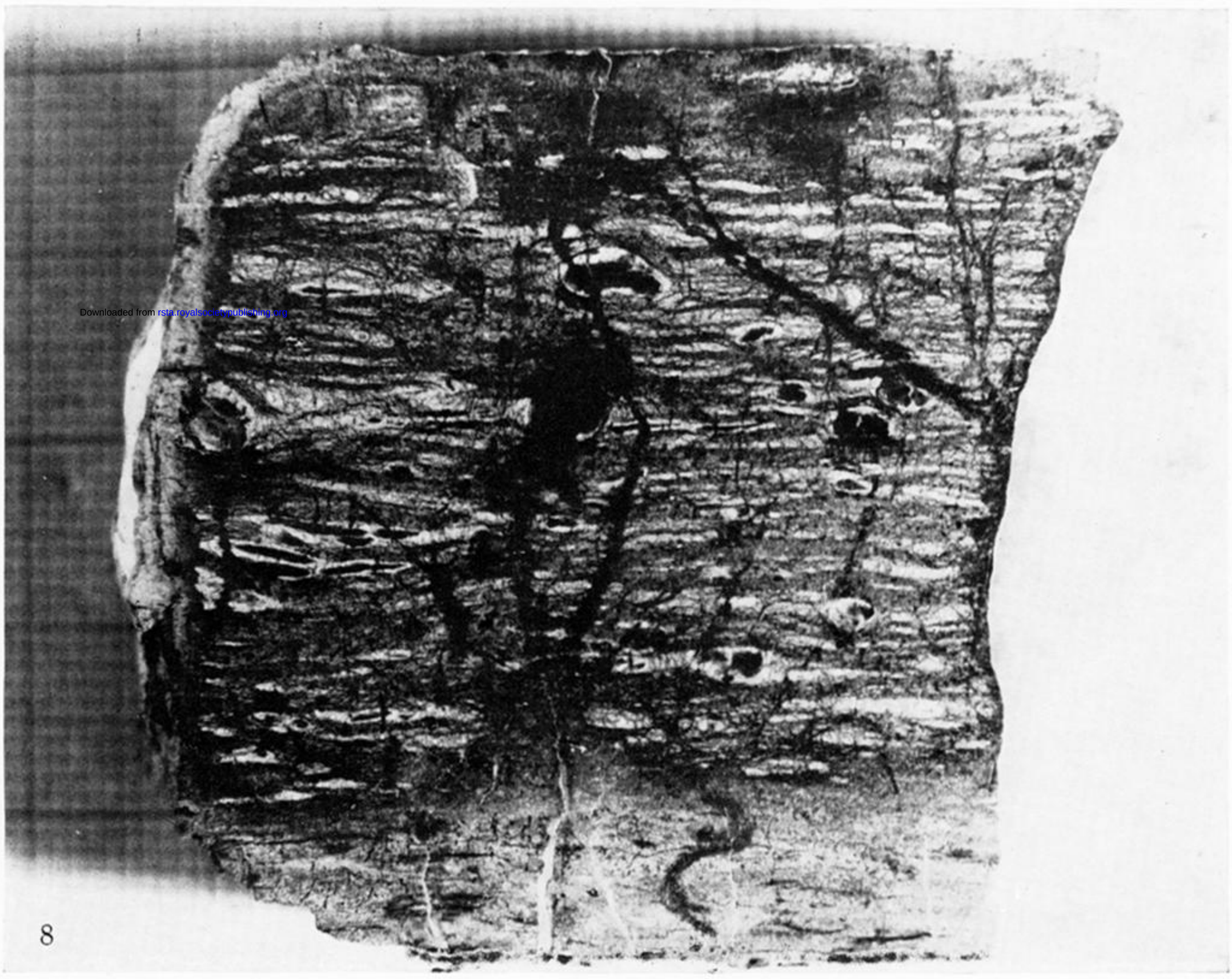

FIGURE 6. Platy lava fragment, quenched on two sides and having a convoluted, unpalagonitized presumably down-facing surface. (*a*) Top and side view; (*b*) Bottom view. Specimen about 18 cm in maximum dimension. Analysed sample (analysis 1, table 2).

FIGURE 7. Rounded and euhedral crystals of plagioclase, and very rarely of olivine, in a pillow basalt from the ridge segment south of the Vema F.Z. (dredge 58, figures 3 and 4, analysed sample, analysis 1, table 2).

FIGURE 8. Partially serpentinized plagioclase peridotite. White areas are weathered olivine; dark areas in matrix are mainly serpentine. Note infiltration of lighter coloured serpentine along bottom joint surface. Large oval, elongated bodies are enstatite porphyroclasts which have high alumina interiors. Sample is about 8 cm wide.